Figure S1

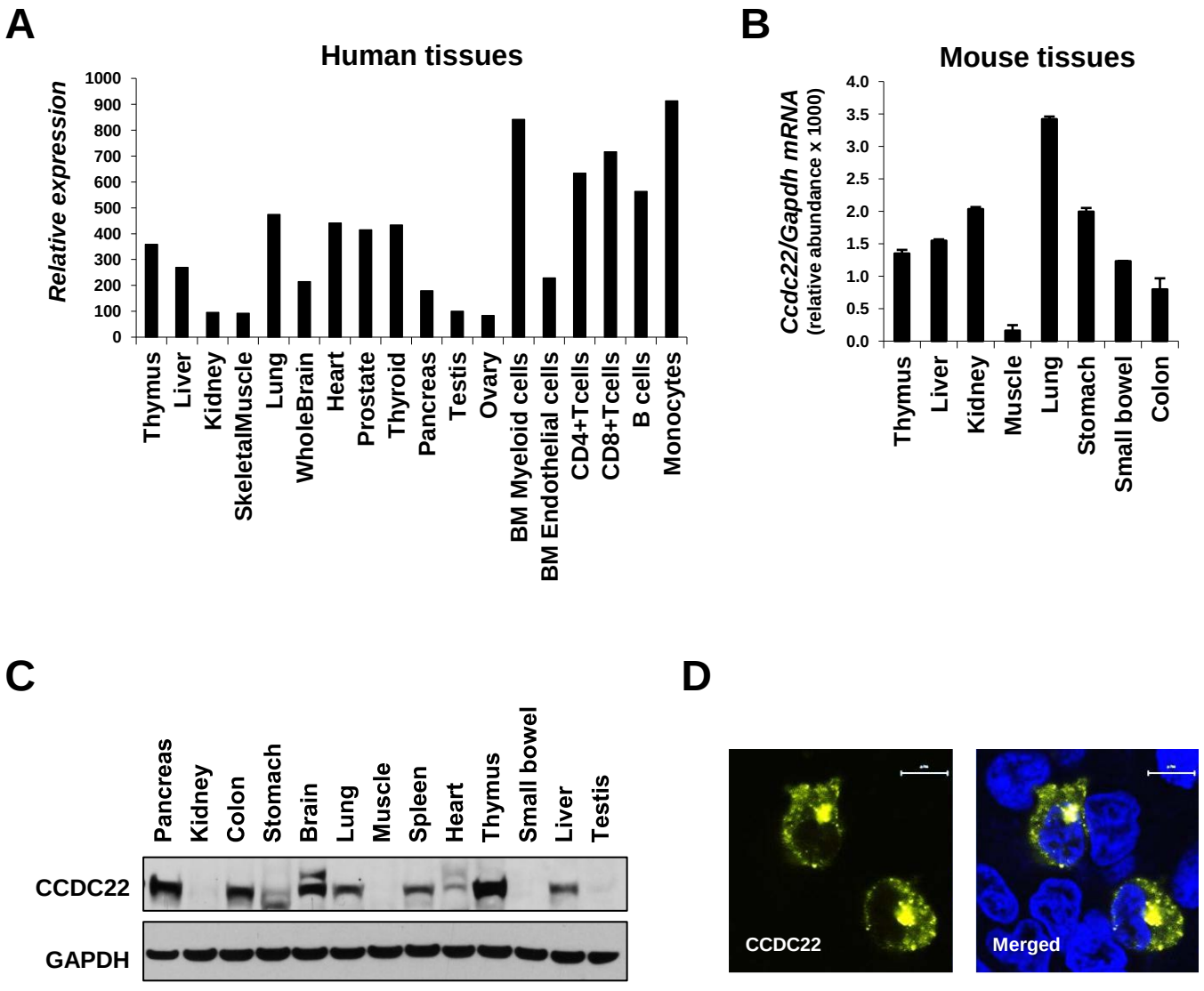

Figure S1: *CCDC22* expression pattern at the tissue and cellular levels. (A) *CCDC22* mRNA expression in human tissues according to oligonucleotide arrays (publicly available from BioGPS). **(B)** Expression of *CCDC22* mRNA in selected mouse tissues was determined by qRT-PCR. **(C)** CCDC22 protein levels in selected mouse tissues was examined by immunoblotting. (**D)** Cellular distribution of CCDC22. CCDC22 fused to yellow fluorescent protein (YFP) was transfected in HeLa cells. Cells were counterstained with Hoechst and imaged in a confocal microscope. The scale bar corresponds to 10 μm.

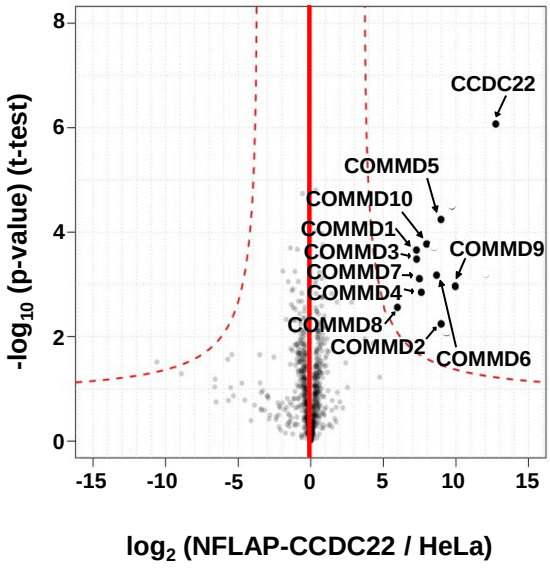

Figure S2: Results of affinity purification of CCDC22. An amino-terminal FLAP tag (NFLAP) was fused to CCDC22. This volcano plot depicts the co-purification of all COMMD proteins with this CCDC22 tagged protein. For each protein identified by mass spectrometry, the ratio of the intensities in the CCDC22 IPs over parental HeLa cell control was calculated and plotted against the p value of the t-test calculated from triplicate experiments, both on a logarithmic scale. The dotted curved lines represent the cutoff calculated based on a false discovery rate estimation. Specific interactors appear in the upper right corner.

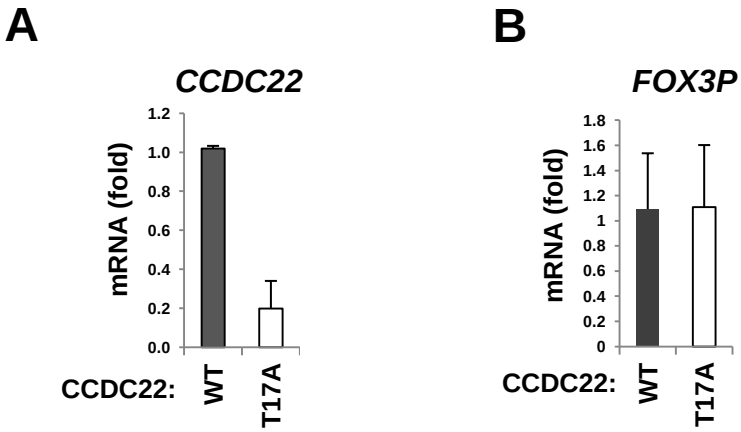

Figure S3: (A) XLID patients have reduced levels of *CCDC22* mRNA. *CCDC22* transcript levels in immortalized lymphoblastoid cell lines (LCLs) derived from an affected individual and a healthy control were analyzed by qRT-PCR. **(B) Level of the *FOXP3* transcript is unaffected in XLID patients.** *FOXP3* mRNA in LCLs derived from an affected individual and a healthy control were analyzed by qRT-PCR.

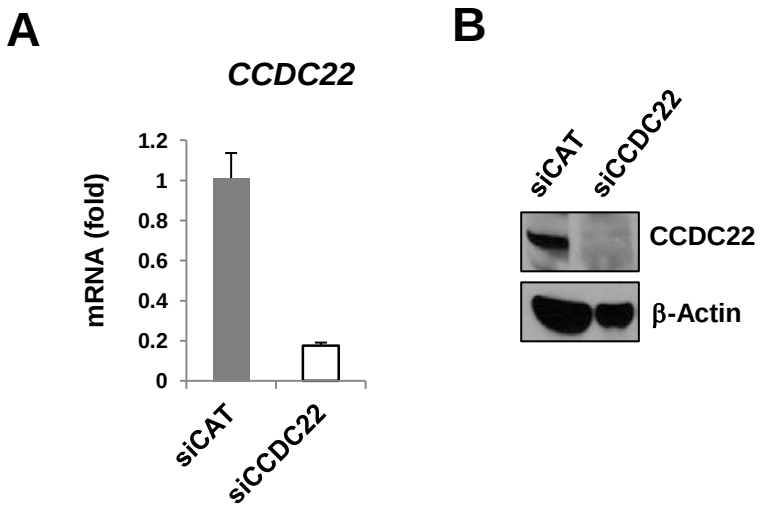

Figure S4: *CCDC22* silencing after siRNA transfection. Lymphoblastoid cells from a healthy donor were transfected with CCDC22 siRNA by electroporation (Figure 4D). CCDC22 levels were analyzed at the mRNA level by qRT-PCR (A) and at the protein level by immunoblotting (B).

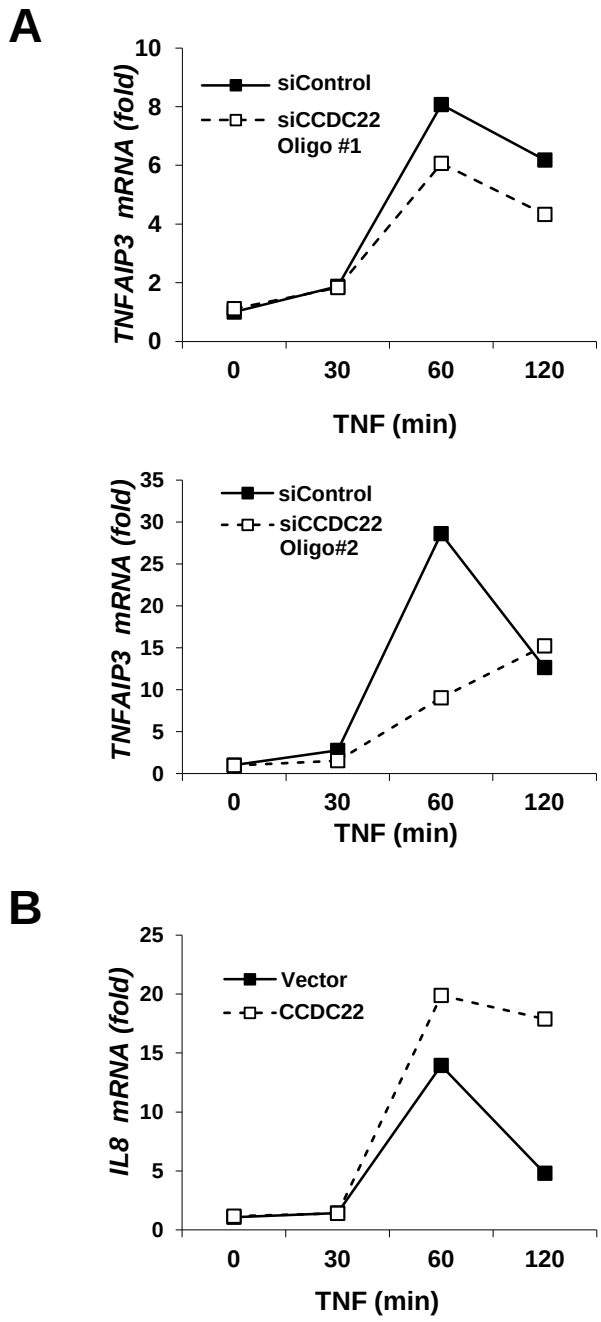

Figure S5: (A) CCDC22 deficiency results in depressed TNF-induced expression of *TNFAIP3*. HEK 293 cells were transfected with the indicated siRNA duplexes and stimulated with TNF. The induction of *TNFAIP3* was determined by qRT-PCR. **(B) *CCDC22* overexpression results in enhanced expression of *IL8*.** Cells transfected with CCDC22 or a vector control were stimulated with TNF. *IL8* mRNA expression was determined by qRT-PCR.

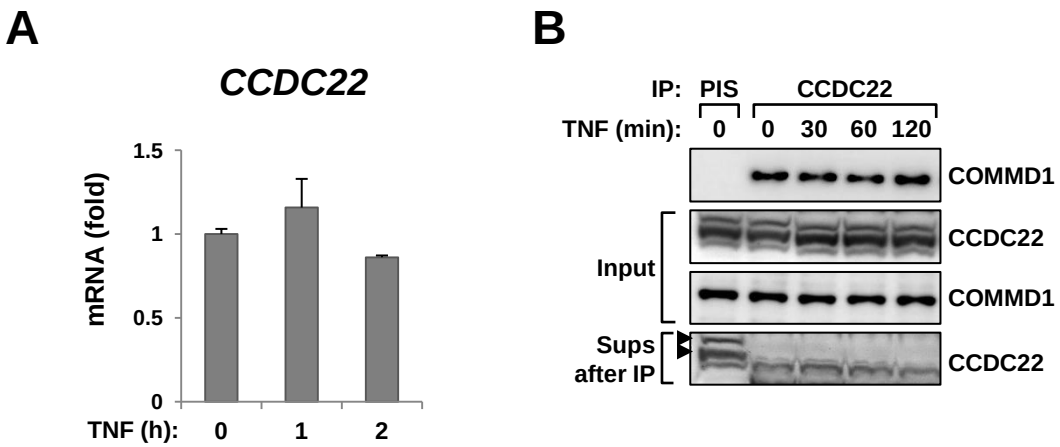

Figure S6: (A) *CCDC22* expression is constitutive and not induced by NF-κB activation. Total mRNA was isolated from non-stimulated and TNF-treated HEK 293 cells. *CCDC22* expression levels were analyzed by qRT-PCR. **(B) CCDC22-COMMD1 interaction does not depend on NF-κB activation.** Endogenous CCDC22 was immunoprecipitated from lysates of non-treated and TNF-treated HEK 293 cells. The recovered material was immunoblotted for endogenous COMMD1. Supernatants (sups) after immunoprecipitation were used as a marker of CCDC22 immunoprecipitation effectiveness. Arrowheads correspond to the CCDC22 bands.

Figure S7

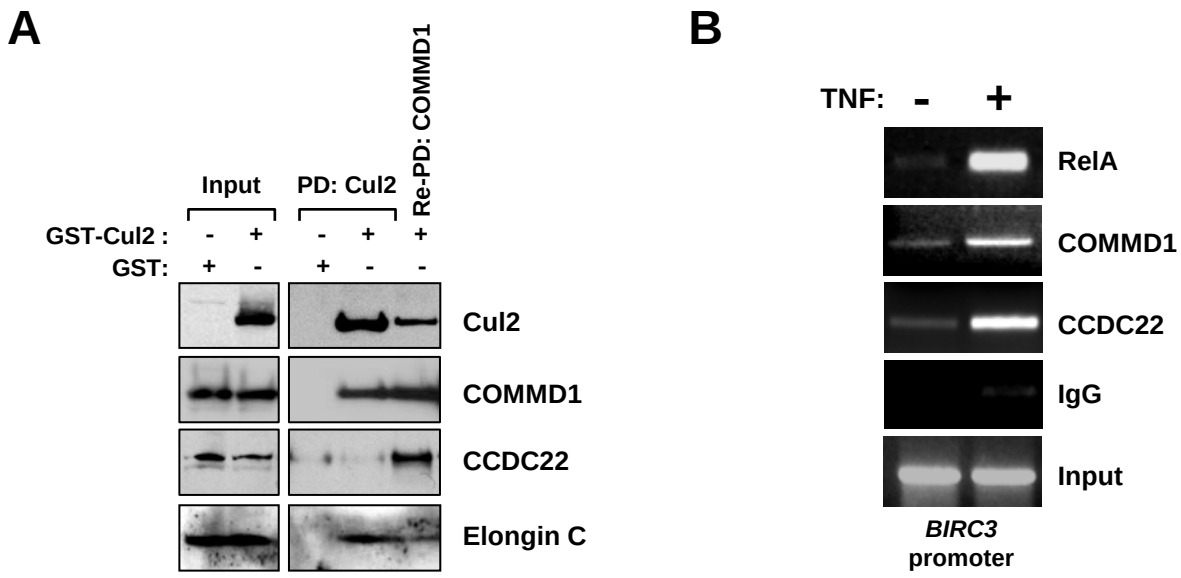

Figure S7: (A) The purified Cul2-COMMD1 complex contains CCDC22. Bimolecular affinity purification of a Cul2-COMMD1 complex was performed. Briefly, GST or Cul2 fused with GST were expressed in HEK 293 cells along with COMMD1 fused to a biotinylation tag. Cul2 was purified through a GSH affinity column and subsequently eluted. COMMD1 was then precipitated from the eluted material using streptavidin agarose beads. The resulting material was immunoblotted for endogenous CCDC22 and Elongin C, as well as for Cul2 and COMMD1. **(B) CCDC22 is recruited to the *BIRC3* promoter**. Chromatin immunoprecipitations were performed using chromatin preparations from unstimulated HEK 293 cells or cells stimulated with TNF for 30 minutes. After immunoprecipitation of the indicated endogenous proteins, recovery of the *BIRC3* promoter region spanning an NF-κB binding site was determined by PCR.

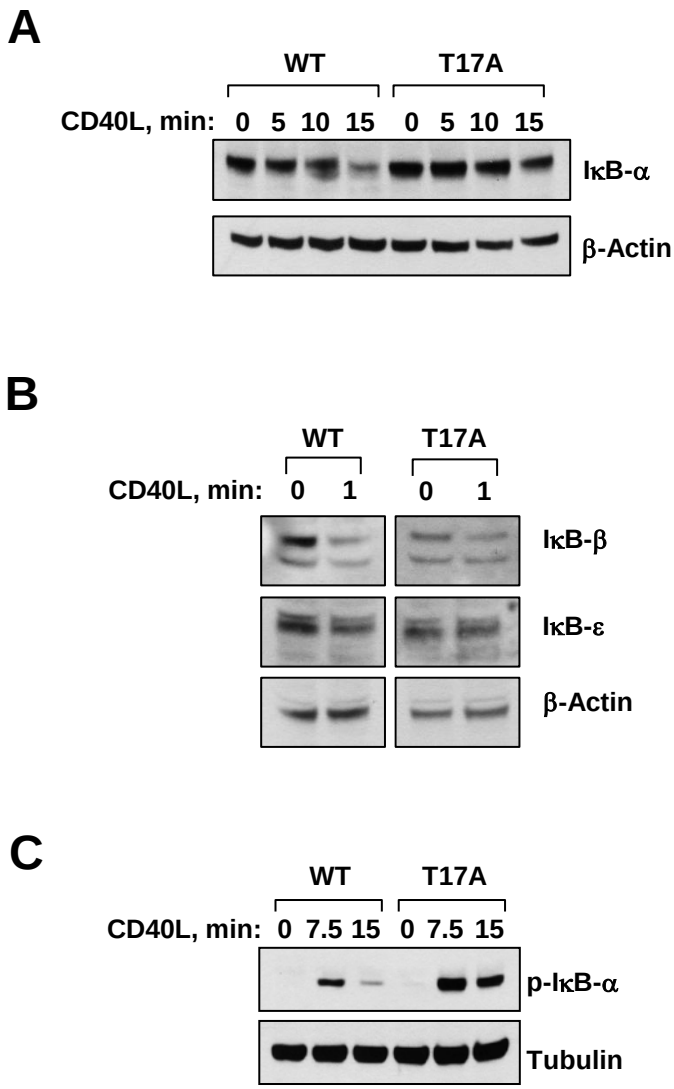

Figure S8: (A), (B), and (C) XLID patients have reduced rate of degradation of IκB proteins. LCLs from a healthy control and an XLID patient were stimulated with CD40L. The degradation dynamics of different IκB proteins was examined by immunoblotting. Phosphorylation of IκB-α in response to CD40L was also ascertained (C).

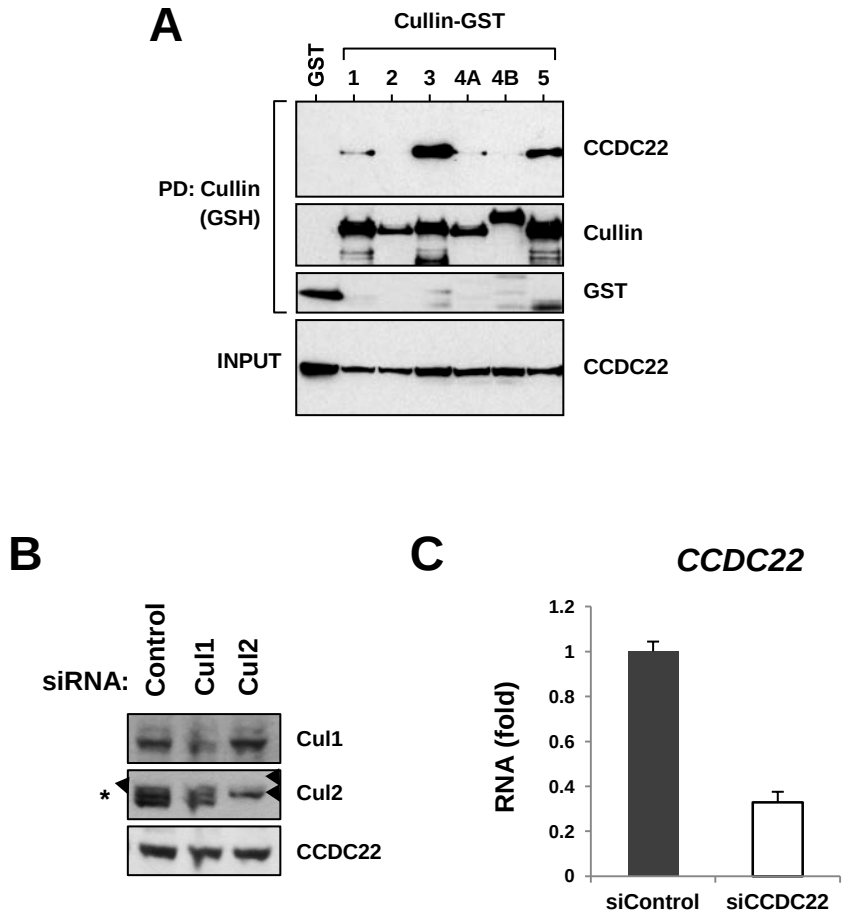

Figure S9: (A) CCDC22 binds to various Cullin proteins. Six canonical Cullins were expressed fused to GST along with FLAG-tagged CCDC22. After precipitation of the Cullin proteins, CCDC22 was detected by immunoblotting. **(B) Silencing of Cul1 and Cul2 after siRNA transfection.** Lysates of cells used in Figure 6D and treated with siRNA control, or against Cul1, or Cul2 were analyzed for protein expression by immunoblotting. CCDC22 is used as loading control; asterisk marks a non-specific band seen with the Cul2 antibody. **(C) CCDC22 silencing after siRNA transfection.** HEK 293 cells were transfected with control or anti-CCDC22 siRNA in Figure 6E. CCDC22 level was analyzed in a representative sample by qRT-PCR.

Table S1: siRNA duplexes utilized

Target	Species	Targeted sequence
CAT, Chloramphenicol acetyltransferase (Control)	Bacteria	TGGAGTGAATACCACGACGAT
CCDC22, #1	Human	CCAAGACTGGTGCTCCTAA
CCDC22, #2	Human	GGAAGGAGGAGGTCTATAA
COMMD1	Human	AAGTCTATTGCGTCTGCAGAC
COMMD8, #1	Human	CTTGTGATGTCTTGACTGT
COMMD8, #2	Human	GAACACTACAGAACTGACA
COMMD10	Human	TGCAATAGATACAGGAAGATT
CUL1	Human	TAGACATTGGGTTCGCCGT
CUL2	Human	GCCAGTCAAGAGCTAGGTT

Table S2: Primers utilized for qRT-PCR (all human genes)

Target	Sense primer	Antisense primer
ACTB	GCGGGAAATCGTGCGTGACATT	GATGGAGTTGAAGGTAGTTTCGTG
CCDC22	CTATCAGAACTTCCTCTACCC	GGAGAATAGCTGAGTCACCT
COMMD1	GCAAATATGGACAGGAATC	CAGAATTTGGTTGACTTTGAC
COMMD8	GTTTGGGAATCAGAAGAATG	GCTGAAATATCTCTTCATCAG
COMMD10	TCTATGGGTCAAGAAACAG	CGGTCTCTAGCTTACAGG
CXCL1	GAAAGCTTGCCTCAATCCTG	CTTCCTCCTCCCTTCTGGTC
IL8	ATGACTTCCAAGCTGGCCGTGGCT	TCTCAGCCCTCTTCAAAAACTTCTC
NFKB2	AGAGGCTTCCGATTTCGATATGG	GGATAGGTCTTTCGGCCCTTC
NFKBIB	CTCCCGACACCAACCATA	CCTCCACTGCCAAATGAA
RELB	CAGCCTCGTGGGGAAAGAC	GCCCAGGTTGTTAAAACTGTGC
TNF	CCTCTCTCTAATCAGCCCTCTG	GAGGACCTGGGAGTAGATGAG
TNFAIP3	ATCATCCACAAAGCCCTCAT	CCTTCCTCAGTACCAAGTCT
FOXP3	GTGGCCCGGATGTGAGAAG	GGAGCCCTTGTCGGATGATG

Table S3: Antibodies utilized in this study

Antibody	Supplier	Cat. No.
α-Tubulin	Molecular Probes	A11126
β-Actin	Sigma	A5441
CCDC22	Sigma	HPA000888
COMMD1	Abnova	H00150684-M01
Cul1	Santa Cruz Biotechnology	sc-11384
Cul2	Zymed	51-1800
FLAG	Sigma	A8592
GAPDH	GeneTex	GT239
GST	Santa Cruz Biotechnology	sc-459
HA	CoVance	MMS101R
IκB-α	Upstate Biotechnology	06-494
IκB-β	Santa Cruz Biotechnology	sc-9130
IκB-ε	Santa Cruz Biotechnology	sc-7155
p50	Upstate Biotechnology	06-886
phospho-IκB-α	Cell Signaling	9246
Rabbit IgG	Cell Signaling	2729
RelA	Santa Cruz Biotechnology	sc-372
RelA	Santa Cruz Biotechnology	sc-8008
RNA Pol II	Santa Cruz Biotechnology	sc-9001
Ubiquitin	Stressgen	SPA-205